

Quantitative analysis of phase formation and growth in ternary mixtures upon evaporation of one component

Stela Andrea Muntean 

Department of Engineering and Physics, Karlstad University, 65188 Karlstad, Sweden

Vì C. E. Kronberg *


Department of Engineering and Physics, Karlstad University, 65188 Karlstad, Sweden

Matteo Colangeli 

Department of Information Engineering, Computer Science and Mathematics, University of L'Aquila, 67100 L'Aquila, Italy

Adrian Muntean 

Department of Mathematics and Computer Science, Karlstad University, 65188 Karlstad, Sweden

Jan van Stam 

Department of Engineering and Chemical Sciences, Karlstad University, 65188 Karlstad, Sweden

Ellen Moons 

Department of Engineering and Physics, Karlstad University, 65188 Karlstad, Sweden

Emilio N. M. Cirillo 

Department of Basic and Applied Sciences for Engineering (SBAI), Sapienza University of Rome, 00161 Rome, Italy



(Received 26 March 2022; revised 20 June 2022; accepted 10 July 2022; published 5 August 2022)

We perform a quantitative analysis of Monte Carlo simulation results of phase separation in ternary blends upon evaporation of one component. Specifically, we calculate the average domain size and plot it as a function of simulation time to compute the exponent of the obtained power law. We compare and discuss results obtained by two different methods, for three different models: two-dimensional (2D) binary-state model (Ising model), 2D ternary-state model with and without evaporation. For the ternary-state models, we study additionally the dependence of the domain growth on concentration, temperature and initial composition. We reproduce the expected $1/3$ exponent for the Ising model, while for the ternary-state model without evaporation and for the one with evaporation we obtain lower values of the exponent. It turns out that phase separation patterns that can form in this type of systems are complex. The obtained quantitative results give valuable insights towards devising computable theoretical estimations of size effects on morphologies as they occur in the context of organic solar cells.

DOI: [10.1103/PhysRevE.106.025306](https://doi.org/10.1103/PhysRevE.106.025306)

I. INTRODUCTION

Morphology formation is one of the key factors in the processing of multicomponent thin films from solution. In applications such as organic solar cells the photoactive layer is

a thin film of electron donor and electron acceptor molecules. The internal structure of the morphology of this layer plays a very important role for the electric charge generation and collection; cf., e.g., [1]. The photoactive layer is produced within a solution with organic solvent, a distinguishing feature of the organic solar cells compared to the more conventional, silicon-based, photovoltaic systems.

Morphologies are formed by phase separation of the electron donor and electron acceptor molecules during the evaporation of the solvent [2,3].

In the framework of this paper, lattice spin systems are used to understand size effects on different morphologies as well as characteristic time scales observed in domain growth phenomena. A paradigmatic model is the widely studied two-dimensional (2D) Ising model [4], that served as a model system for the investigation of phase separation in magnetic

*Present address: Department of Mathematics and Computer Science, Eindhoven University of Technology, Eindhoven, 5600 MB, The Netherlands.

Published by the American Physical Society under the terms of the [Creative Commons Attribution 4.0 International](https://creativecommons.org/licenses/by/4.0/) license. Further distribution of this work must maintain attribution to the author(s) and the published article's title, journal citation, and DOI. Funded by [Bibsam](https://www.bibsam.nl/).

materials and of novel transport mechanisms under nonequilibrium conditions [5]. For such a model, it has been well established that in the spinodal decomposition regime, namely for zero external field and subcritical temperature, the average diameter of the formed domains scales with time as a power law, where the exponents depend on the details of the dynamics. For nonconservative and conservative dynamics the exponents are $1/2$, and respectively, $1/3$; see, e.g., [6]. Interestingly, these results were shown to be robust with respect to slight modifications of the Hamiltonian describing the equilibrium properties of the system; we refer the reader, for instance, to [7]. On the other hand, different interesting phenomena are observed when the dynamics are modified more drastically by introducing, for example, shear effects as in [8].

In order to describe the formation of internal structures in the presence of an evaporating solvent as typical to applications in the context of organic solar cells, a three-state model is needed. Two straightforward generalisations of the Ising model with nearest neighbor interaction between three-state spin variables are the Blume-Capel [9–11] and the Potts [12] models. Both these models have received much attention for their ability to model different physical situations both at equilibrium [13] and out of equilibrium [14–17]. The distinguishing feature between these two models is that in the Blume-Capel model, interfaces between different spins have different costs. The dynamics of phase separation for the Potts model seen in the spinodal decomposition regime are not completely understood: a rather clear scenario is described for nonconservative dynamics for three- and four-state spins [18], whereas the understanding is only partial when spin variables with larger cardinality are considered [19]. To the authors' knowledge, no references are available for the Potts nor the Blume-Capel model with conservative dynamics.

Three-state lattice models were used in [20] and [21] as an efficient tool to study phase separation patterns in ternary mixtures that allow the evaporation of one of the components as an alternative to phase-field models used in the same context [22–25]. In our previous work [20], we focused our attention on exploring the relevant parameters that influence the morphology formation. This is a subject of large interest in the community and was discussed in many experimental and computational studies [22–24, 26–34]; see also [35] for related work done for stochastic models for competitive growth of phases.

In the present work, the emphasis falls onto the quantitative analysis of the results for relevant choices of parameters. Quantitative studies are important particularly when one wants to compare morphologies obtained with different computational models or to compare computational and experimental results. In general, different models and computational methods give results on different length scales. In some approaches the characteristic length scales are incorporated into the model parameters, such as the parameters arising in the structure of the interaction potential for atomistic molecular simulations. Even in apparently scale-free models, the nature of the modeling assumptions induces a length scale range for the results. Having in view potential applications of our three-state lattice models, it is of a primary concern to identify relevant quantities that capture the essence of domain size evolution across the scales.

The quantitative analysis presented here is an important step towards a more general quantification and eventual classification of morphology pictures obtained by different experimental and computational methods.

In this paper, we follow up the ideas developed in our previous work [20] and give a quantitative study of the phase-separated domains using a slightly simplified version of our original model generalizing the Blume-Capel and Potts models. The three possible states of the spin variable are denoted here by -1 , 0 , and $+1$: “ 0 ” is interpreted as solvent molecules, whereas “ ± 1 ” represent the other two components. In a real system the properties of the molecules, such as the molecular weight of the polymers, have a significant effect on the resulting film morphology and ultimately on the performance of the polymer solar cell [36–38]. Here we prefer the above mentioned more general formulation, since we do not take into account the different molecular weights of the three components or the volumes they occupy and hence each site occupies the same volume in the lattice. In the case where the molecular weights of the three components are comparable, the spin variables could be interpreted as different molecules, but in our case of interest, where the nonevaporating molecules, e.g., polymers, have different sizes and are much larger than the solvent molecules, a more general interpretation is needed. In our model, lattice sites are associated with volumes filled with substance, i.e., molecules of one of the components of the ternary system. The morphology is determined to a large extent by the molecular interactions represented by the interaction matrix J , whose elements, in principle, could be adjusted according to experimental evidence [22] or molecular simulations [39]. Even if spin lattice systems are simplified models that do not fully capture all aspects of real molecular interacting systems, they can reproduce bulk heterojunction morphologies reasonably well and are commonly used in the field [40, 41].

To study the phase separation in the ternary mixture upon evaporation of one of the components, we consider a spin model with a Kawasaki-like dynamics [42] governed by the Metropolis algorithm [43] to account for energy differences associated to possible spin exchanges and computed using appropriate boundary conditions. The Kawasaki dynamics is modified here such that evaporation of the 0 component is allowed. Keeping track of the solvent evaporation is crucial for the study of the morphology formation in solution-borne thin films, used, e.g., in the preparation of the active layer in organic photovoltaics. To implement such a mechanism, the zeros in the first row of the lattice are removed (evaporation) and replaced by a $+1$ or a -1 with probability chosen proportionally to the initial fractions. The dynamics start with a randomly chosen configuration consisting of a fixed fraction of the three different spin species and evolve until an *a priori* small concentration of solvent is reached. The problem we study is related to the spinodal decomposition with the new ingredient of the evaporation of the zero component. We have to keep in mind that our model relies on assumptions and will not correspond to all aspects of the physical reality and that further improvements are possible to make the model more realistic. This falls outside the scope of the present work.

The model will be studied by means of Monte Carlo simulations and the size of the growing domains will be estimated

via correlation function and structure factor methods. Several other techniques have been proposed and used in the past literature, including renormalization group techniques. We refer to [6] for a wide overview of methods, techniques, and results in this area of research.

The paper is organized as follows: we first define the model and describe the tools that we rely on to investigate the domain formation under evaporation. Then we discuss our numerical results first in the absence of the evaporation, and then, when the evaporation of the solvent, i.e., of the zero component, is involved. After discussing the effect of the temperature parameter on the overall system dynamics, a short summary of our findings concludes the paper.

II. MODEL AND METHODS

In this section we first define the model and then illustrate the tools that we use to measure the domain growth. In the last part of this section, we briefly illustrate these methods by discussing the standard Ising case. For more details on the Monte Carlo method and its variations, we refer the reader, e.g., to the monographs [44,45].

A. Model

Let Λ be the square $\{1, \dots, L\}^2$ endowed with periodic boundary conditions, where L is the lateral size of the simulation box expressed in lattice points. An element of Λ is called a *site* and two sites are said to be *nearest neighbors* if their Euclidean distance is one. A pair of nearest neighboring sites is called a *bond*. We associate the *spin variable* $\sigma(x, y) \in \{-1, 0, +1\}$ with each site $(x, y) \in \Lambda$ and define the total *energy* using the *Hamiltonian*

$$H(\sigma) = \frac{1}{2} \sum_{\substack{(x,y), (x',y') \in \Lambda: \\ |(x,y)-(x',y')|=1}} J_{\sigma(x,y)\sigma(x',y')}, \quad J = \begin{bmatrix} 0 & 1 & 4 \\ 1 & 0 & 1 \\ 4 & 1 & 0 \end{bmatrix}, \quad (1)$$

for any configuration $\sigma \in \{-1, 0, +1\}^\Lambda$, where the elements $J_{\alpha,\beta}$, with $\alpha, \beta = -1, 0, 1$, are organized in the matrix J such that the row and the column indices take the values $-1, 0, +1$.

In this case, there is no cost associated with self-interaction (the main diagonal of J), a relatively small cost between ± 1 and 0 sites, and a relatively large cost of an interface between -1 and $+1$. Such a choice of interaction matrix corresponds to a well-studied parametrization of the Blume-Capel model with zero magnetic field and zero chemical potential; see, e.g., [14,15,17]. Note that this specific structure of the interaction matrix J promotes the phase separation of the components, irrespective of the presence or absence of the evaporation.

Consider the integer time variable $t \geq 0$, that will be expressed in Monte Carlo Sweeps (MCS) [44,45]. Fix the parameter $\beta > 0$ and refer to $1/\beta$ as the *temperature*. Fix $c_{-1}, c_0, c_{+1} \in [0, 1)$ with the constraint $c_{-1} + c_0 + c_{+1} = 1$. They are the corresponding fractions of $-1, 0$, and $+1$ spins in the initial configuration, that is at time $t = 0$. In the case of the two-state model and three-state model without evaporation, we follow a classical Kawasaki dynamics for the Ising model and Blume-Capel model, respectively. In the case of the

three-state model with evaporation, the stochastic evolution σ_t is constructed by repeating at each time $t > 0$ the following steps L^2 times:

- (i) Choose a bond at random with uniform probability
- (ii) If the bond is of the type $((x, L), (x, 1))$ and $\sigma(x, L) = 0$, then replace the spin zero at the site (x, L) by $+1$ with probability $c_{+1}/(1 - c_0)$ and by -1 with probability $1 - c_{+1}/(1 - c_0) = c_{-1}/(1 - c_0)$ (say that the zero *evaporated*)
- (iii) Otherwise, let Δ be the difference of energy between the configuration obtained by exchanging the spins at the two sites of the bond and the actual configuration; exchange the two spins at the sites of the bond with probability 1 if $\Delta < 0$ and with probability $\exp\{-\beta \Delta\}$ if $\Delta \geq 0$.

We stop the dynamics when the total number of zeros in the system becomes smaller than $L^2/10$, hence at $c_0 = 0.1$. Based on this description, the dynamics are of Kawasaki type complemented with a Metropolis updating rule with the addition of the evaporation rule (i.e., step ii) of the algorithm).

B. Methods

A common measure of the average domain size is obtained by fixing a cutoff for the *two-point correlation function*. More precisely, for any $s \in \{s_x, s_y\}$ let

$$G(s, t) = \frac{1}{L^2} \sum_{(x,y) \in \Lambda} \sigma_t(x, y) \sigma_t(x + s_x, y + s_y) \quad (2)$$

be the two-point correlation function. Moreover, we also consider the horizontal and vertical two-point correlation functions $G_x(r, t) = G((r, 0), t)$ and $G_y(r, t) = G((0, r), t)$, where r is an integer number. The direction-dependent two-point correlation functions typically decrease from their maximum value at $s = 0$ in an oscillatory fashion, such that it is possible to estimate the size of the domains by fixing a cutoff and finding the value at which the two correlation function intersect such a cutoff. In this way, we shall find an estimate for the horizontal and vertical diameters of the domains, R_x and R_y , respectively.

Another well-established domain-size measurement is based on the first momenta of the *structure factor*. More precisely, for any (k_x, k_y) in the first Brillouin zone $\{-\pi, -\pi + 2\pi/L, \dots, \pi - 2\pi/L, \pi\}^2$, let

$$C((k_x, k_y), t) = \frac{1}{L^2} \left| \sum_{(x,y) \in \Lambda} \sigma_t(x, y) e^{i(k_x x + k_y y)} \right|^2 \quad (3)$$

be the structure factor. Note that the quantity in the absolute value above is simply the Fourier transform of the configuration at Monte Carlo time t , and can thus be evaluated using any form of fast Fourier transform technique to speed up execution. Hence, another way of estimating the horizontal and the vertical diameters of the domains is by redefining R_x and R_y as follows:

$$R_\alpha = \frac{\sum_{(k_x, k_y)} C((k_x, k_y), t)}{\sum_{(k_x, k_y)} |k_\alpha| C((k_x, k_y), t)}, \quad (4)$$

where $\alpha \in \{x, y\}$ and each summation is carried out over the first Brillouin zone.

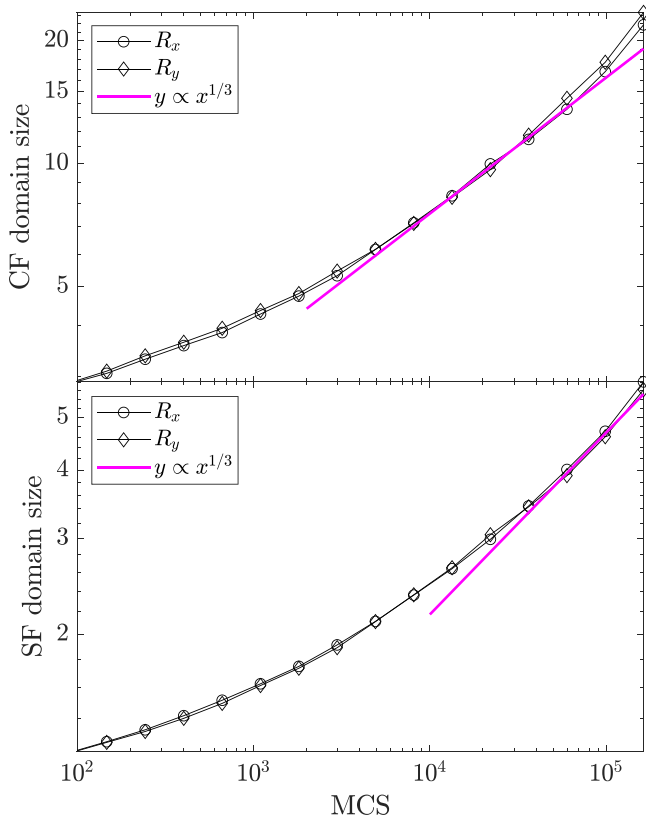


FIG. 1. Single history for the Kawasaki Ising dynamics with $L = 512$ and $\beta = 1.0$. Correlation function measure and structure factor measure of the horizontal and vertical domain size in the upper and lower panel, respectively. Circles and diamonds refer, respectively, to R_x and R_y . The purple line gives the $x^{1/3}$ slope.

C. Domain growth in the 2D Ising model

As a test of this methodology, we consider the classical 2D Ising model under Kawasaki dynamics, for which the growth exponent of $1/3$ has been extensively verified; we refer the reader, for instance, to the works [6,7]. The results for our case are shown in the left and right panel of Fig. 1. Here we report the resulting domain growth of the same run as evaluated using both the correlation function and the structure factor. The previously established $1/3$ exponent is recovered, lending credit to the chosen methodology.

Based on Fig. 1, we note that the two methods yield quite similar power-law structures, i.e., the same exponent with different constant prefactors. This yields a discrepancy in the absolute values of the domain sizes calculated based on these two methods. Since we do not have a physically imposed length scale (i.e., no physical meaning of length is included in our lattice models), this is not a critical distinction. It is more important to observe how the domains grow, hence we wish to compare the exponents in the power laws mainly at long times. Sometimes, also short timescales could be of interest if power laws of suitable observables are detected.

Both the correlation function and structure factor measure show that two different regimes can be distinguished: the initial one in which the domains start to be formed by coalescence of equal spins and the second one, characterized by the

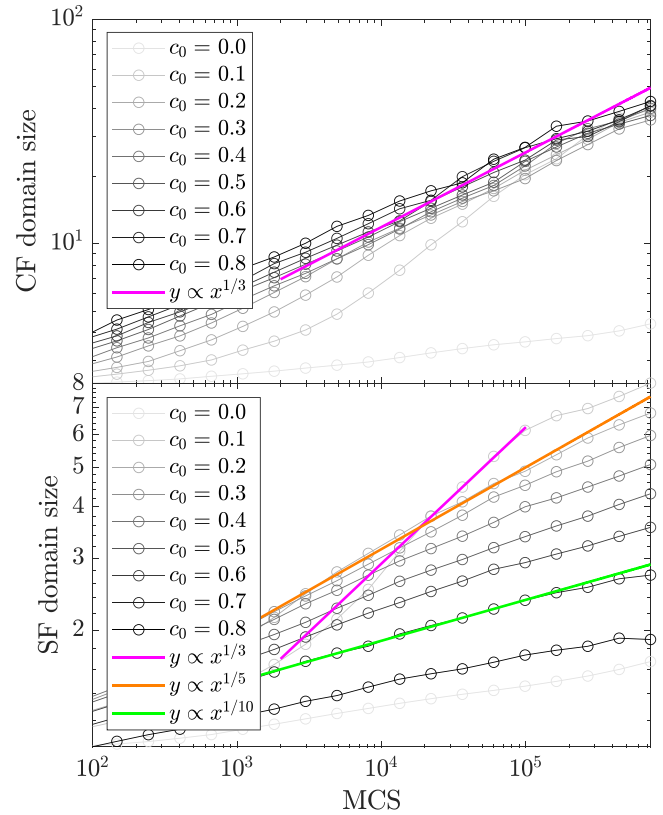


FIG. 2. Three-state model with $L = 512$ and $\beta = 1.0$. Estimate of the horizontal domain size via two-point correlation function and structure factor in the upper and lower panel, respectively. One single system history for each solvent concentration c_0 is considered. Different colors refer to different values of the concentration of zeros, $c_0 = 0.0, 0.1, \dots, 0.8$ from light to dark. The purple, orange, and green lines give, respectively, the $x^{1/3}$, $x^{1/5}$, and $x^{1/10}$ slope.

power-law scaling, in which the already formed domains grow in time. This last regime will be addressed as the *growing* or *scale invariant* regime.

III. NUMERICAL RESULTS

After having checked the validity of the different methodologies on the Kawasaki Ising dynamics, we now study the three-state model introduced above. We explore the model for different choices of the initial fraction of zeros c_0 . For all the simulations, we set $c_{-1} = c_{+1}$, so that the initial number of minuses and pluses will be equal. Due to the evaporation mechanism, the ratio between minuses and pluses will oscillate slightly during the overall evolution, while the fraction of zeros will progressively decrease.

A. Domain growth in the three-state model without evaporation

The results for the growth of domains obtained with the two different methods for calculating R_x from the same Monte Carlo simulation of the three-state model are shown in Fig. 2. We omit to show the results for R_y as in the absence of evaporation domains are isotropic, as in the Ising case (see Fig. 1). Data for different values of the initial zeros concentration c_0 are reported here. The connecting lines between the data

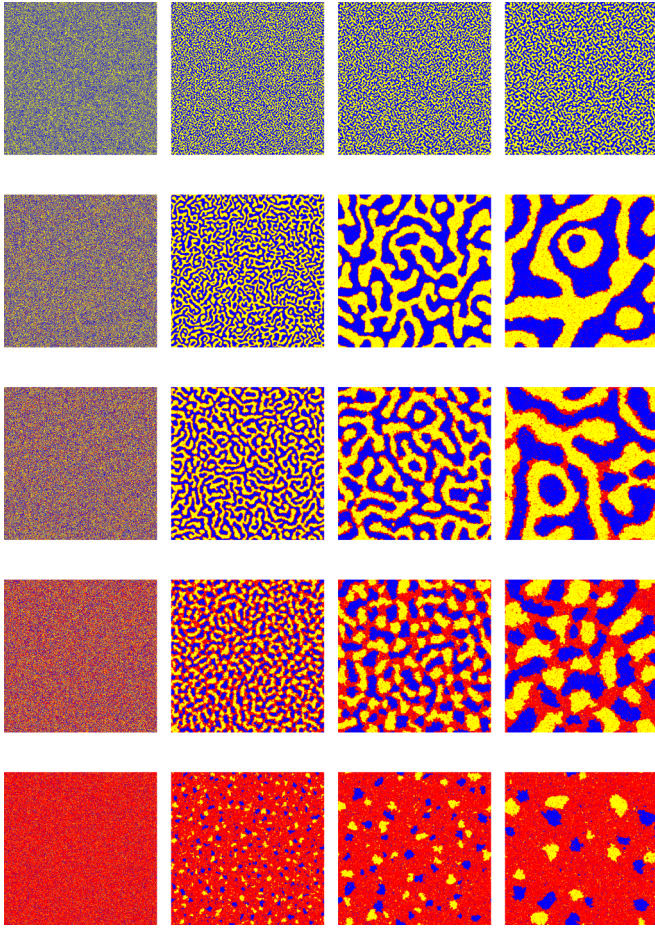


FIG. 3. Morphology formation and domain coarsening of the three-state model without evaporation for $L = 512$ and $\beta = 1.0$. From the top to the bottom $c_0 = 0.0, 0.1, 0.2, 0.4, 0.8$. From the left to the right $t = 0, 8102, 98714, 729415$ MCS.

points do not imply piecewise linear regression. The $x^{1/3}$ line is shown as reference, since a $1/3$ exponent of the power law for the domain size as a function of time is the observed behavior in the scale-invariant regime via the correlation function (left panel). This is consistent with the findings for a conserved dynamics as reported in [6].

The two panels show that in the two-state case, namely, for $c_0 = 0$, growth is very slow and in the time interval considered in the simulation, domains have just started to form. This simply means that the scaling regime has not yet been reached, and that the overall process is still in its incipient phase. This line of reasoning is supported by comparing the configurations shown in the upper two rows of Fig. 3. Indeed, looking at the first row, configurations referring to the case $c_0 = 0.0$ are shown. They point out clearly that the growth regime has not yet started, compared to the second row with $c_0 = 0.1$, where the domains have grown substantially.

Both analysis techniques agree when predicting that the domain growth is much faster when a moderate amount of zeros is present in the system. This situation is not unprecedented in literature; see, e.g., [46] where the authors demonstrate a process of greatly speeding up the Ising Kawasaki dynamics by introducing one or several vacancies in

the lattice. We argue that the zero component of the three-state model acts as a form of vacancy, since its interface cost is smaller. Hence, replacing it by a -1 or by a $+1$ spin is cheaper. Thus, zero sites are more mobile and greatly speed up the dynamics. Indeed, for $c_0 = 0.1$, which is reported in the second row of the same figure, the domain formation started at about 10^3 MCS. This is also very well confirmed by the data in the right panel of Fig. 2: the curve referring to the case $c_0 = 0.1$ mildly grows until 10^3 MCS where it experiences an abrupt change of the slope to a growth regime with the exponent $1/3$.

Both the correlation function and the structure factor measure characteristic domain sizes. Interestingly, they give different results for $c_0 \geq 0.2$; see again Fig. 2. The correlation function-based measure is compatible with a $1/3$ exponent in the scaling regime for all values of c_0 . On the other hand, the structure factor-based measure suggests that growth is slower when the zeros concentration is increased. The configurations plotted in the lower three rows of Fig. 3 indicate that the growth mechanisms change when more zeros are present. In the second row of Fig. 3 zeros form a thin film around plus and minus domains, so that growth happens essentially as in a two-state lattice system. This is a typical situation observed in the Blume-Capel model, see also the behavior in the metastable regime studied in [14] where the nucleation of the stable phase is realized via the formation of a critical droplet in which the minuses are separated by the pluses by a thin layer of zeros. As usual in lattice spin models, interfaces are characterized by a sharp behavior, in contrast to what happens in other contexts, such as phase models and lattice Boltzmann systems [47], where diffuse interfaces are observed.

In the plots provided in the lower three rows of Fig. 3 the situation is rather different: domains of zeros have sizes comparable with pluses and minus ones. Furthermore, the three species seem to compete during growth. In the last row, when the zero concentration is very high, the process seems to become more peculiar, in the sense that plus and minus domains grow inside a connected background of zeros. It is worth mentioning that similar behaviors have been observed in different regimes, specifically in the study of the metastability occurring in the framework of the Blume-Capel model [14–17], when growth does not happen via the coalescence of small droplets but rather via a sudden nucleation of a large droplet.

The fact that different values of the zeros concentration give rise to different growing mechanisms suggests that, for this three-state system, the way in which the structure factor measures the size of the domains is more reliable than that provided by the correlation function technique. Even if, from the experimental point of view, this case might seem less interesting, our results can be related to situations where the concentration of the active components in the solvent does not vary much, as it would be, for instance, the case for a certain short amount of time at the bottom of the film or for a very slow evaporation.

B. Domain growth in the three-state model with evaporation

Now we discuss our results for the domain growth in the presence of the evaporation, which is the most interesting case

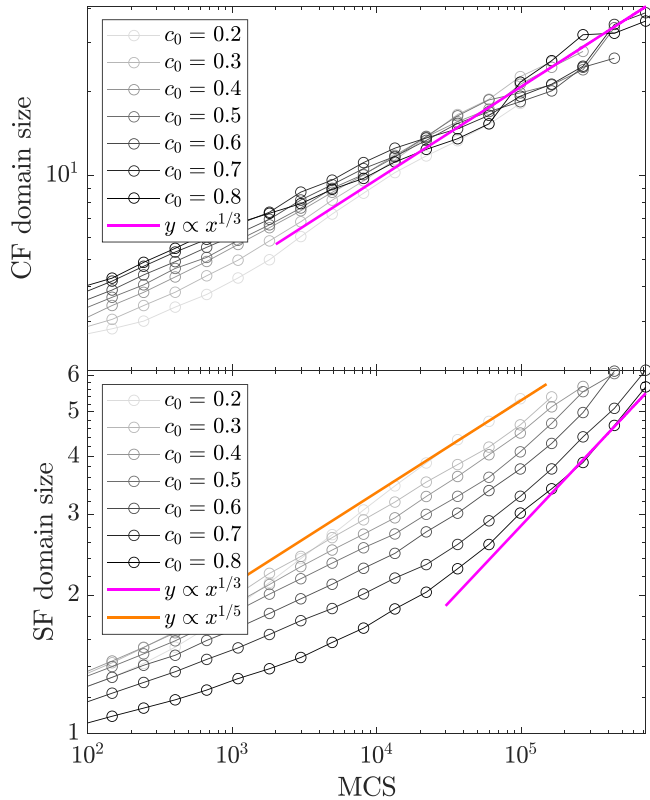


FIG. 4. Horizontal domain size-based measure via the correlation function (upper panel) and the structure factor computation (lower panel) for the three-state lattice model with evaporation for $L = 512$ and $\beta = 1.0$. One single system history per initial concentration. Different colors refer to different values of the concentration of zeros, $c_0 = 0.2, 0.3, \dots, 0.8$ from light to dark. The purple and the orange lines give, respectively, the $x^{1/3}$ and $x^{1/5}$ slope.

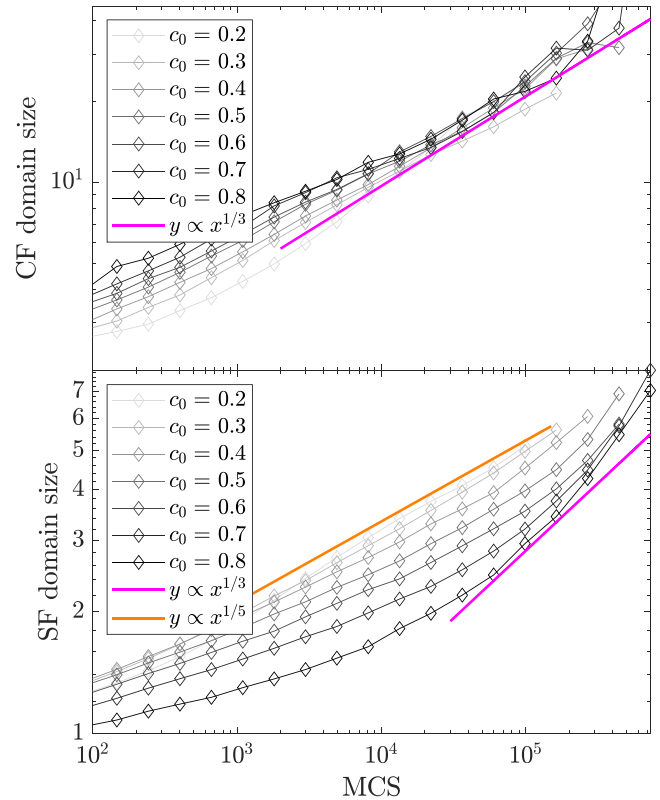


FIG. 5. As in Fig. 4 for the vertical domain size.

in terms of applications to ternary mixtures in the context of organic solar cells referred to in the introduction. The horizontal and vertical domain sizes measured with the correlation function and with the structure factor are reported in Fig. 4 and Fig. 5, respectively. Just like in the case discussed in the previous section, the two-point correlation function shows a domain growth exponent of $1/3$ in the appropriate regime, while the structure factor method gives a more complex behavior, showing growth exponents between $1/5$ and $1/3$ for R_x . What concerns R_y , we see briefly a growth exponent of $1/3$, which then speeds up further near the end of the evaporation. This asymmetry is not necessarily surprising as this problem is anisotropic due to the evaporation of the zeros at the top row of the lattice.

Even in the presence of evaporation, the growth mechanism seems to depend on the solvent concentration; see Fig. 6. Note that the last frame (for 729 415 MCS) is missing for the first two initial concentrations of zeros, as the length of the simulation is decided by the final concentration of zeros (recall the stopping condition for the dynamics is when $c_0 = 0.1$) and, in these cases, that value is reached for shorter simulation lengths. By similar arguments as before, it is believed that the structure factor yields the most meaningful domain size calculation, which is further supported by the observation that

$R_y > R_x$ near the end of the evaporative process (compare Fig. 4 and Fig. 5). This also appears to be the case when looking at the final configurations in Fig. 6, and it is thus believed to be a good indicator of the validity of the domain size calculations.

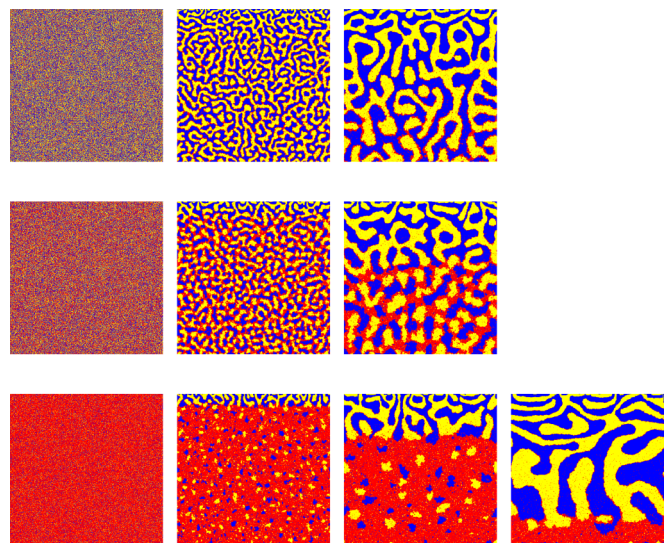


FIG. 6. Morphology formation and domain coarsening of the three-state lattice model with evaporation for $L = 512$ and $\beta = 1.0$. From the top to the bottom $c_0 = 0.2, 0.4, 0.8$. From the left to the right $t = 0, 8102, 98\,714, 729\,415$ MCS.

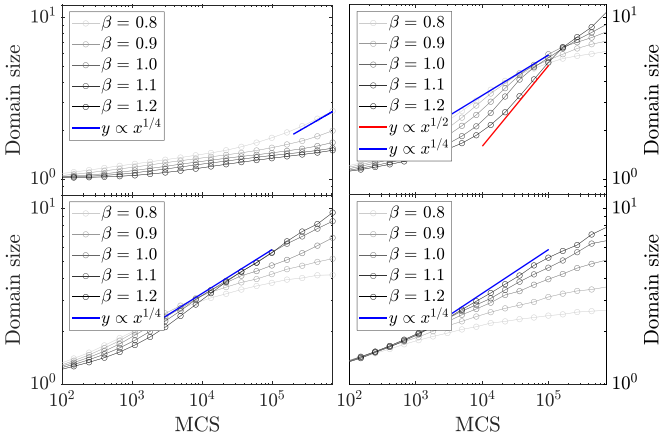


FIG. 7. Structure factor estimate of horizontal domain size for the three-state lattice model without evaporation for $c_0 = 0.0$ (upper row, left), $c_0 = 0.1$ (upper row, right), $c_0 = 0.2$ (lower row, left), and $c_0 = 0.4$ (lower row, right) for different values of the temperature (see inset). Different colors refer to different values of the inverse temperature, $\beta = 0.8, 0.9, \dots, 1.2$ from light to dark. The blue and the green lines give, respectively, the $x^{1/4}$ and $x^{1/2}$ slope.

C. Effect of temperature

Temperature is an important factor in the context of our lattice models as well as for the actual experimental processing of the thin film, both in the initial phase of the solvent evaporation, but also in the late stages and even for after processing, via thermal annealing. Direct comparisons of the simulation results with experiment are not feasible at this stage due to lack of temperature controlled in-situ experimental data especially at early stages but also due to the qualitative character of the temperature in our model, captured only in terms of β^{-1} . Nevertheless, we can see clear tendencies on the domains growth and this is a good starting point for further investigations. In this section, we investigate the effect the temperature β^{-1} has on the domains growth as they are formed in the context of the three-state lattice model without and with evaporation. The estimates of the domains size are done via the structure factor method.

In Fig. 7 we plot our result in absence of evaporation. Several noteworthy aspects appear. With a binary ± 1 mixture, namely, $c_0 = 0.0$ (see the left top panel in the figure), it is clear that increasing temperature (decreasing β) is associated with accelerating dynamics. As the concentration of zeros is increased, this behavior becomes more complex. More specifically, the initial trend is still comparable, i.e., increasing temperature can be associated with larger domains after the same time. At larger times, this is no longer the case; see the time slice $\sim 10^5$ MCS in the top right panel of Fig. 7, where the $\beta = 1.2$ data cross the $\beta = 0.8$ one. As the solvent concentration continues to increase, the effect of the temperature diminishes before the inflection point (which also occurs at earlier times, bringing evidence to the idea that the third species speeds up the dynamics). Finally, for $c_0 = 0.6$, the inflection point is no longer visible in the current time domain; see the right bottom panel in Fig. 7.

It is instructive to look for a moment at the morphology formation exhibited in Fig. 8 for the case $c_0 = 0.4$. Note that

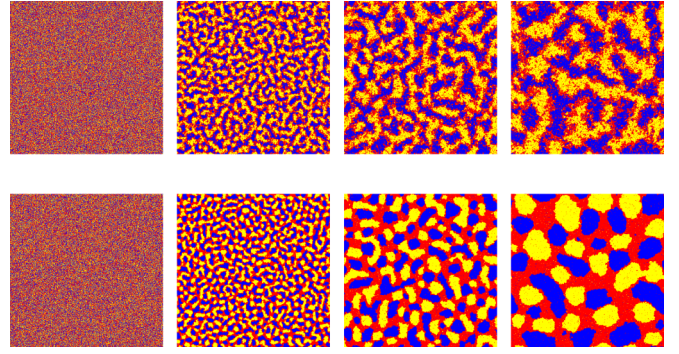


FIG. 8. Morphology formation, and domain coarsening of the three-state lattice model without evaporation for $L = 512$, $c_0 = 0.4$, $\beta = 0.8$ (top row), and $\beta = 1.2$ (bottom row). From left to right: $t = 0, 8102, 98714, 729415$ MCS.

for a high temperature ($\beta = 0.8$), the zero sites (depicted in red) readily penetrate the minus- and plus-filled domains (the yellow and blue regions), to the point where the interface boundaries are rather difficult to identify. When the temperature is low (e.g., for $\beta = 1.2$), the situation is significantly different, and the phases are clearly defined, with minimal interpenetration. It is difficult to say by inspection that the domains are larger in terms of area in the second case (i.e., lower row in Fig. 8), but it is clear that they are more well defined. Since the Fourier transform is quite sensitive to the sharpness of the boundaries of the domains, this will affect the results in Fig. 7 in the sense that results for high β are more accurate compared to those for low β .

We further consider the effect of temperature when the zeros evaporate through the top row of the lattice; see Fig. 9. These data appear consistent with the case without evaporation at least from the point of view that the initial behavior is similar. At longer times, the evaporation effects dominate, and the domain coarsening deviates from scenarios computed with the three-state lattice model without evaporation. Here again we observe the inflection point, but only in the first row of Fig. 9, indicating that the dynamics are further accelerated due to the evaporation.

A proposed mechanism explaining the inflection points in Fig. 7 and Fig. 9 is the following: high temperatures and/or high ratio of ± 1 sites favors the growth of the domains. This seems to hold until a certain critical domain size is reached, after which both the increase in temperature, and hence, increase in fluctuations allow the zeros to penetrate the domains more easily. Consequently, this leads to an altering of the average domain size.

IV. CONCLUDING REMARKS AND FURTHER RESEARCH

In this work, we proposed a quantitative analysis of phase formation and domain growth in ternary mixtures, both with conservative and nonconservative dynamics. In the latter case, one component is evaporated from the top of the lattice in a process akin to that utilized in the fabrication of solution borne thin films used in photovoltaics applications based on organic solar cells. We reproduce the $1/3$ exponent for the Ising model, while for the ternary-state model without

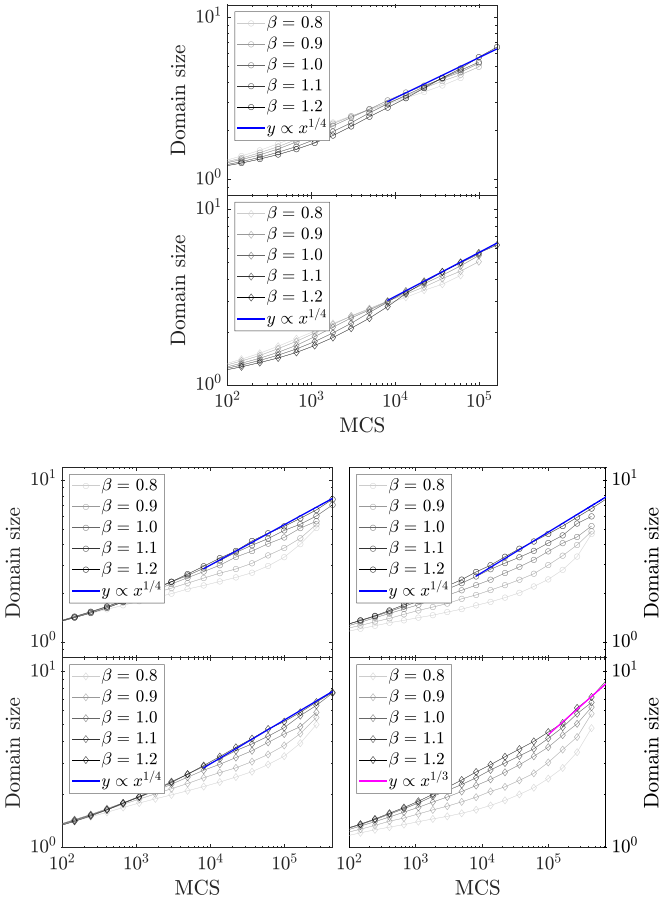


FIG. 9. Structure factor estimate of horizontal (each lower subpanel) and vertical (each upper subpanel) domain size for the three-state model with evaporation for $c_0 = 0.2, 0.4, 0.6$ (upper, left, and right two panels, respectively) for different values of the temperature, $\beta = 0.8, 0.9, \dots, 1.2$ from light to dark. The blue and the purple lines give, respectively, the $x^{1/4}$ and $x^{1/3}$ slope.

evaporation and for that with evaporation we obtain lower values of this exponent. Estimating how domains grow is a quite complex task—in our context, it is heavily influenced by the initial mixture concentration as well as by the temperature. Interestingly, note that the morphologies obtained in the present simulations can be found as well in experimentally built thin films; see, e.g., [22,48].

Further research

Suggestions for further research include an extension to three dimensions for improved applicability to experiments and to validate the two-dimensional results by studying a slice of the morphology. Understanding three-dimensional effects is indeed our next target and short time plan, as such a setting would allow direct comparison with experimentally obtained morphologies.

Even in two dimensions, one could conceive a number of interesting avenues of research, such as the further investigation of the influence of changes to the interaction matrix J and extending the model to a more physically relevant one by taking into account the different molecular weights and

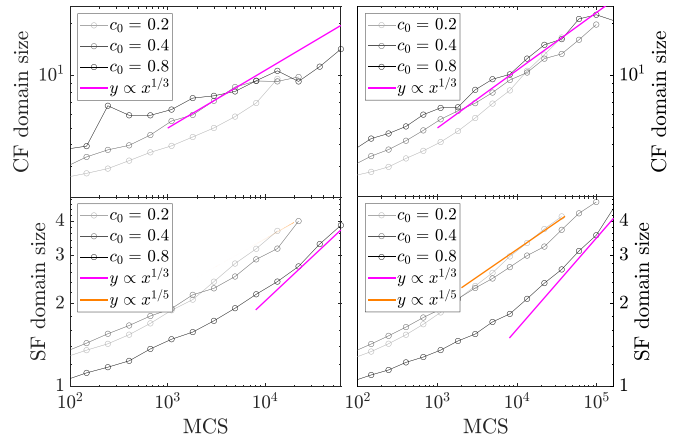


FIG. 10. Horizontal domain size-based measure via the correlation function (upper row) and the structure factor computation (lower row) for the three-state lattice model with evaporation for $\beta = 1.0$, $L = 128$ (left column), $L = 256$ (right column). One single system history per initial concentration. Different colors refer to different values of the concentration of zeros, $c_0 = 0.2, 0.4, 0.8$ from light to dark. The purple and the orange lines give, respectively, the $x^{1/3}$ and the $x^{1/5}$ slope.

volumes of the substance. In the introduction section, we referred to the experimental situation that raised the domain size question we are addressing here. Monitoring the domain size evolution experimentally during film formation requires *in situ* techniques that can monitor the formation of structures directly or indirectly as a function of drying time [49–51]. Another approach to capture early stages of the phase separation is to prepare the evaporating films under microgravity conditions and then simulate numerically those scenarios. Alike investigation routes will be studied elsewhere.

ACKNOWLEDGMENTS

This work was partially funded by the Swedish National Space Agency, Grant No. 174/19, and the Knut och Alice Wallenbergs Stiftelse, Grant No. 2016.0059. V.C.E.K. acknowledges the Lericci Foundation for the travel grant to the University of L’Aquila. Computational resources were

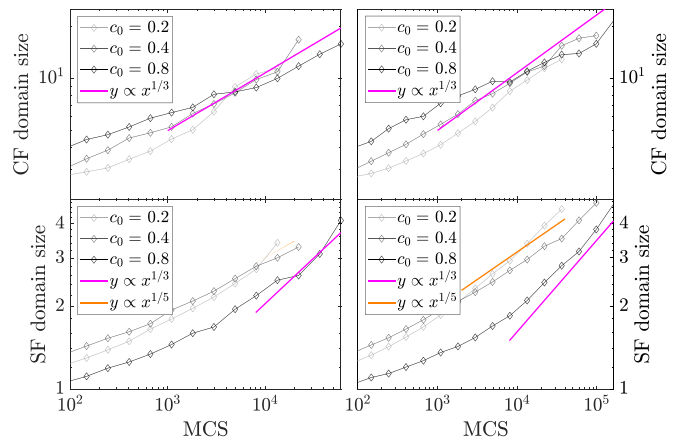


FIG. 11. As in Fig. 10 for the vertical domain size.

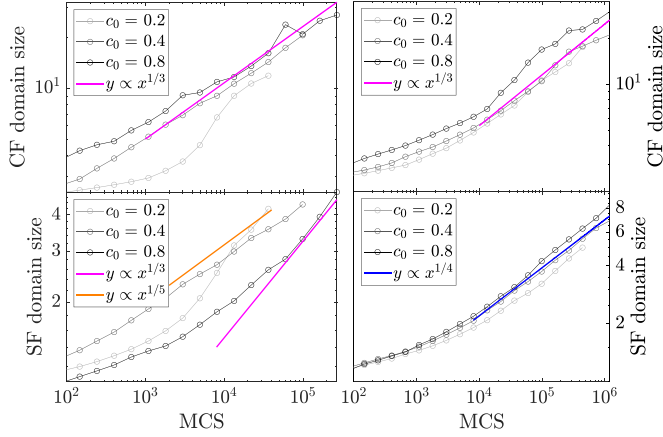


FIG. 12. Horizontal domain size-based measure via the correlation function (upper row) and the structure factor computation (lower row) for the three-state lattice model with evaporation for $\beta = 1.0$, $L = 256$, interaction J_1 (left column), and interaction J_2 (right column). One single system history per initial concentration. Different colors refer to different values of the concentration of zeros, $c_0 = 0.2, 0.4, 0.8$ from light to dark. The purple, the blue and the orange lines give, respectively, the $x^{1/3}$, $x^{1/4}$ and the $x^{1/5}$ slope.

provided by projects SNIC 2019-7-48, SNIC 2020-5-664, and SNIC 2021-1-46 at the Swedish National Infrastructure for Computing (SNIC), partially funded by the Swedish Research Council through Grant Agreement No. 2018-05973.

APPENDIX: SENSITIVITY WITH RESPECT TO L AND J

We check if the growth behaviors discussed above are sensible with respect to the choice of the lattice size L and the interaction J . We expect no dependence on L , while we cannot exclude that the details of the growth will depend even on slight modifications of the structure of the matrix J . Indeed, as we mentioned in the Introduction and in the Further Research sections, we think that the interaction matrix can be used to encode some physical properties of the system which can influence the growth rates.

For what concerns L , we have repeated some of the measures for smaller values of the lattice size, namely, $L =$

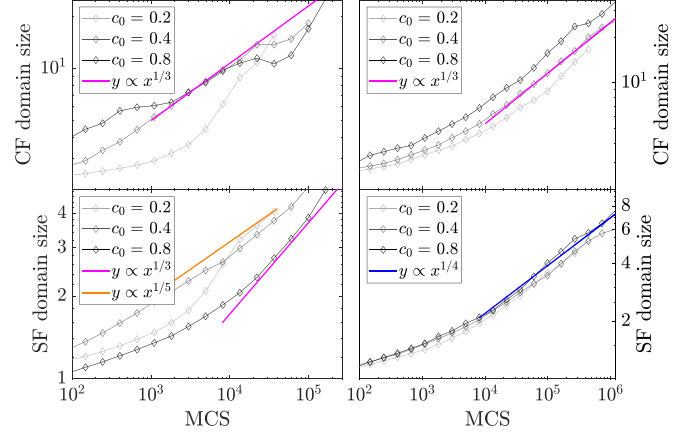


FIG. 13. As in Fig. 12 for the vertical domain size.

128, 256 and, as shown in Fig. 10 and Fig. 11 the same behaviors observed for $L = 512$ are found; see Fig. 4 and Fig. 5. It is worth mentioning that the simulation data for $L = 128$ are clearly lower in resolution compared to higher values of L .

For what concerns the dependence of the growth behavior on the details of the interaction J , we have considered the two possible choices,

$$J_1 = \begin{bmatrix} 0 & 1 & 6 \\ 1 & 0 & 1 \\ 6 & 1 & 0 \end{bmatrix} \text{ and } J_2 = \begin{bmatrix} 0 & 2 & 4 \\ 2 & 0 & 2 \\ 4 & 2 & 0 \end{bmatrix}, \quad (\text{A1})$$

and we have repeated the measures as those reported in Fig. 4 and Fig. 5 on a lattice with $L = 256$. The new interactions have been chosen by keeping the same structure as in J : the energy cost of a direct interface between -1 and $+1$ spins is kept larger than that of interfaces involving zero spins, but we have modified the relative magnitudes of the energy costs. As shown in Fig. 12 and Fig. 13, we found for J_1 similar results to those obtained for J , while for J_2 we found again a growth factor $x^{1/3}$ via the correlation function technique, whereas the structure factor calculation seems to be consistent with a $x^{1/4}$ growth rate.

- [1] F. Zhao, C. Wang, and X. Zhan, Morphology control in organic solar cells, *Adv. Energy Mater.* **8**, 1703147 (2018).
- [2] K. Dalnoki-Veress, J. A. Forrest, J. R. Stevens, and J. R. Dutcher, Phase separation morphology of spin-coated polymer blend thin films, *Physica A* **239**, 87 (1997).
- [3] S. Walheim, M. Böltau, J. Mlynek, G. Krausch, and U. Steiner, Structure formation via polymer demixing in spin-cast films, *Macromolecules* **30**, 4995 (1997).
- [4] L. Onsager, Crystal statistics. I. A two-dimensional model with an order-disorder transition, *Phys. Rev.* **65**, 117 (1944).
- [5] M. Colangeli, C. Giardinà, C. Giberti, and C. Vernia, Nonequilibrium two-dimensional Ising model with stationary uphill diffusion, *Phys. Rev. E* **97**, 030103(R) (2018).
- [6] A. J. Bray, Theory of phase-ordering kinetics, *Adv. Phys.* **43**, 357 (1994).
- [7] E. N. M. Cirillo, G. Gonnella, and S. Stramaglia, Anisotropic dynamical scaling in a spin model with competing interactions, *Phys. Rev. E* **56**, 5065 (1997).
- [8] E. N. M. Cirillo, G. Gonnella, and G. P. Saracco, Monte Carlo results for the Ising model with shear, *Phys. Rev. E* **72**, 026139 (2005).
- [9] M. Blume, Theory of the first-order magnetic phase change in UO_2 , *Phys. Rev.* **141**, 517 (1966).
- [10] M. Blume, V. J. Emery, and R. B. Griffiths, Ising model for the λ transition and phase separation in He^3 - He^4 mixtures, *Phys. Rev. A* **4**, 1071 (1971).

- [11] H. W. Capel, On possibility of first-order phase transitions in Ising systems of triplet ions with zero-field splitting, *Physica* **32**, 966 (1966).
- [12] R. B. Potts, Some generalized order-disorder transformations, *Proc. Cambridge Philos. Soc.* **48**, 106 (1952).
- [13] F. Y. Wu, The Potts model, *Rev. Mod. Phys.* **54**, 235 (1982).
- [14] E. N. M. Cirillo and E. Olivieri, Metastability and nucleation for the Blume-Capel model. Different mechanisms of transition, *J. Stat. Phys.* **83**, 473 (1996).
- [15] E. N. M. Cirillo and F. R. Nardi, Relaxation height in energy landscapes: An application to multiple metastable states, *J. Stat. Phys.* **150**, 1080 (2013).
- [16] E. N. M. Cirillo, F. R. Nardi, and C. Spitoni, Sum of exit times in a series of two metastable states, *Eur. Phys. J.: Spec. Top.* **226**, 2421 (2017).
- [17] C. Landim and P. Lemire, Metastability of the two-dimensional Blume-Capel model with zero chemical potential and small magnetic field, *J. Stat. Phys.* **164**, 346 (2016).
- [18] C. Sire and S. N. Majumdar, Correlations and Coarsening in the q -State Potts Model, *Phys. Rev. Lett.* **74**, 4321 (1995).
- [19] M. Ibáñez de Berganza, E. E. Ferrero, S. A. Cannas, V. Loreto, and A. Petri, Phase separation of the Potts model in the square lattice, *Eur. Phys. J.: Spec. Top.* **143**, 273 (2007).
- [20] E. N. M. Cirillo, M. Colangeli, E. Moons, A. Muntean, S. A. Muntean, and J. van Stam, A lattice model approach to the morphology formation from ternary mixtures during the evaporation of one component, *Eur. Phys. J.: Spec. Top.* **228**, 55 (2019).
- [21] M. Setta, V. C. E. Kronberg, S. A. Muntean, E. Moons, J. van Stam, E. N. M. Cirillo, M. Colangeli, and A. Muntean, A mesoscopic lattice model for morphology formation in ternary mixtures with evaporation, [arXiv:2106.01427](https://arxiv.org/abs/2106.01427) (2021).
- [22] J. Michels and E. Moons, Simulation of surface-directed phase separation in a solution-processed polymer/PCBM blend, *Macromolecules* **46**, 8693 (2013).
- [23] C. Schäfer, J. J. Michels, and P. van der Schoot, Structuring of thin-film polymer mixtures upon solvent evaporation, *Macromolecules* **49**, 6858 (2016).
- [24] O. J. J. Ronsin, D. J. Jang, H.-J. Egelhaaf, C. J. Brabec, and J. Harting, A phase-field model for the evaporation of thin film mixtures, *Phys. Chem. Chem. Phys.* **22**, 6638 (2020).
- [25] O. J. J. Ronsin, D. J. Jang, H.-J. Egelhaaf, C. J. Brabec, and J. Harting, Phase-field simulation of liquid-vapor equilibrium and evaporation of fluid mixtures, *ACS Appl. Mater. Interfaces* **13**, 55988 (2021).
- [26] L. Meng, Y. Shang, Q. Li, Y. Li, X. Zhan, Z. Shuai, R. G. E. Kimber, and A. B. Walker, Dynamic Monte Carlo simulation for highly efficient polymer blend photovoltaics, *J. Phys. Chem. B* **114**, 36 (2010).
- [27] C. Battaile, The kinetic Monte Carlo method: Foundation, implementation, and application, *Comput. Methods Appl. Mech. Eng.* **197**, 3386 (2008).
- [28] E. Bänsch, S. Basting, and R. Krahl, Numerical simulation of two-phase flows with heat and mass transfer, *Discrete Cont. Dyn. Syst. A* **35**, 2325 (2014).
- [29] J. Cummings, J. S. Lowengrub, B. G. Sumpter, S. M. Wise, and R. Kumar, Modeling solvent evaporation during thin film formation in phase separating polymer mixtures, *Soft Matter* **14**, 1833 (2018).
- [30] C. Du, Y. Ji, J. Xue, T. Hou, J. Tang, S.-T. Lee, and Y. Li, Morphology and performance of polymer solar cell characterized by DPD simulation and graph theory, *Sci. Rep.* **5**, 16854 (2015).
- [31] B. P. Lyons, N. Clarke, and C. Groves, The relative importance of domain size, domain purity and domain interfaces to the performance of bulk-heterojunction organic photovoltaics, *Energy Environ. Sci.* **5**, 7657 (2012).
- [32] B. P. Lyons, N. Clarke, and C. Groves, The quantitative effect of surface wetting layers on the performance of organic bulk heterojunction photovoltaic devices, *J. Phys. Chem. C* **115**, 22572 (2011).
- [33] C. Schäfer, S. Paquay, and T. C. B. McLeish, Morphology formation in binary mixtures upon gradual destabilisation, *Soft Matter* **15**, 8450 (2019).
- [34] V. Negi, O. Wodo, J. J. van Franeker, R. A. J. Jansen, and P. A. Bobbert, Simulating phase separation during spin coating of a polymer-fullerene blend: A joint computational and experimental investigation, *ACS Appl. Energy Mater.* **1**, 725 (2018).
- [35] M. Deijfen, O. Häggström, and J. Bagley, A stochastic model for competing growth on \mathbb{R}^d , *Markov Proc. Related Fields* **10**, 217 (2004).
- [36] P. Schilinsky, U. Asawapirom, U. Scherf, M. Biele, and C. J. Brabec, Influence of the molecular weight of poly(3-hexylthiophene) on the performance of bulk heterojunction solar cells, *Chem. Mater.* **17**, 2175 (2005).
- [37] A. M. Ballantyne, L. Chen, J. Dane, T. Hammant, F. M. Braun, M. Heeney, W. Duffy, I. McCulloch, D. D. C. Bradley, and J. Nelson, The effect of poly(3-hexylthiophene) molecular weight on charge transport and the performance of polymer: Fullerene solar cells, *Adv. Funct. Mater.* **18**, 2373 (2008).
- [38] B. Fan, L. Ying, Z. Wang, B. He, X.-F. Jiang, F. Huang, and Y. Cao, Optimisation of processing solvent and molecular weight for the production of green-solvent-processed all-polymer solar cells with a power conversion efficiency over 9%, *Energy Environ. Sci.* **10**, 1243 (2017).
- [39] K. Do, M. K. Ravva, T. Wang, and J.-L. Brédas, Computational methodologies for developing structure-morphology-performance relationships in organic solar cells: A protocol review, *Chem. Mater.* **29**, 346 (2017).
- [40] M. C. Heiber and A. Dhinojwala, Efficient Generation of Model Bulk Heterojunction Morphologies for Organic Photovoltaic Device Modeling, *Phys. Rev. Applied* **2**, 014008 (2014).
- [41] R. Volpi and M. Linares, Organic solar cells, *Chem. Modell.* **13**, 1 (2016).
- [42] K. Kawasaki, Kinetics of Ising model, in *Phase Transitions and Critical Phenomena*, edited by C. Domb and M. S. Green (Academic Press, London, New York, 1972), Vol. 2, pp. 443–501.
- [43] N. Metropolis, A. W. Rosenbluth, M. N. Rosenbluth, A. H. Teller, and E. Teller, Equation of state calculations by fast computing machines, *J. Chem. Phys.* **21**, 1087 (1953).
- [44] M. E. J. Newman and G. T. Barkema, *Monte Carlo Methods in Statistical Physics* (Clarendon Press, Oxford, 2001).
- [45] D. P. Landau and K. Binder, *A Guide to Monte Carlo Simulations in Statistical Physics* (Cambridge University Press, Cambridge, 2009).
- [46] P. Fratzl and O. Penrose, Kinetics of spinodal decomposition in the Ising model with vacancy diffusion, *Phys. Rev. B* **50**, 3477 (1994).

- [47] G. Falcucci, G. Bella, G. Chiatti, S. Chibbaro, M. Sbragaglia, and S. Succi, Lattice Boltzmann models with mid-range interactions, *Commun. Comput. Phys.* **2**, 1071 (2007).
- [48] M. Sprenger, S. Walheim, A. Budkowski, and U. Steiner, Hierarchic structure formation in binary and ternary polymer blends, *Interface Sci.* **11**, 225 (2003).
- [49] Y. Liu, A. Yangui, R. Zhang, A. Kiligaridis, E. Moons, F. Gao, O. Inganäs, I. G. Scheblykin, and F. Zhang, In situ optical studies on morphology formation in organic photovoltaic blends, *Small Methods* **5**, 2100585 (2021).
- [50] M. Buchhorn, S. Wedler, and F. Panzer, Setup to study the in situ evolution of both photoluminescence and absorption during the processing of organic or hybrid semiconductors, *J. Phys. Chem. A* **122**, 9115 (2018).
- [51] B. Schmidt-Hansberg, M. F. G. Klein, K. Peters, F. Buss, J. Pfeifer, S. Walheim, A. Colsmann, U. Lemmer, P. Scharfer, and W. Schabel, *In situ* monitoring the drying kinetics of knife coated polymer-fullerene films for organic solar cells, *J. Appl. Phys.* **106**, 124501 (2009).